

MAJOR PAPER

Performance of a Flexible 12-Channel Head Coil in Comparison to Commercial 16- And 24-Channel Rigid Head Coils

YingJie Kang¹, YiLei Chen¹, JieMing Fang², YanWen Huang¹,
Hui Wang¹, ZhiGang Gong¹, SongHua Zhan¹, and WenLi Tan^{1*}

Purpose: To compare the performance of a 12-channel flexible head coil (HFC12) with commercial 16-channel (HRC16) and 24-channel (HRC24) rigid coils.

Methods: The phantom study was performed on a 1.5 T MR scanner with HFC12, HRC16, and HRC24. The SNR and noise correlation matrix of T1WI, T2WI, and diffusion weighted imaging (DWI) were measured. The SNR profiles were created according to the SNR. In addition, 1/g-factors were calculated in different acceleration directions. In the *in vivo* study, T1WI, T2WI, and DWI were performed in one healthy volunteer with three different coils. The SNR and noise correlation matrix were measured.

Results: In the phantom study and *in vivo* study, the SNR of HFC12 in the transverse, sagittal, and coronal planes was the highest, followed by HRC24, and that of HRC16 was the lowest. The SNR profiles showed that the SNR at the edge of HFC12 was the highest. The mean value of the noise correlation matrix of HFC12 was the highest. The 1/g-factor results showed that HFC12 obtained the best acceleration ability in the head-foot acceleration direction when the reduction factor was set to two. The SNR of HFC12 in most cortices was significantly higher than that of HRC16 and HRC24, except in the occipital cortex. The SNR of HRC24 in the occipital cortex was higher than that of HFC12.

Conclusion: The SNR of HFC12 in T1WI, T2WI, and DWI was better than that of the HRC24 and HRC16. The SNR of HFC12 in the cortex was significantly higher than that of the commercial rigid head coil, except in the occipital cortex.

Keywords: head coil, performance, magnetic resonance imaging, signal-to-noise ratio, acceleration ability

Introduction

MR RF coils are an important part of MR and directly affect the temporal resolution, spatial resolution, and uniformity of images.¹ The MR coils can be either rigid or flexible. At present, the head coils used in clinical examinations are typically rigid, easy to carry, and not affected by the patients'

posture. However, the inner diameter of the rigid coil is fixed, which results in decreased image quality if the diameter of the individual's head is significantly smaller than that of the coil. In contrast, a flexible coil is typically used for imaging extremities and joints. Such a coil is scalable and can be form-fitted according to the size and shape of the individual's body parts. Furthermore, the SNR of images will be improved due to closer proximity to the individual.^{2,3} In addition, a flexible coil is suitable for special posture imaging, especially for individuals with limited range of motion due to trauma of the head and neck or those who need to be in the prone position to undergo head imaging. Some sequences, such as blood oxygenation level-dependent functional MRI (fMRI), sacrifice spatial resolution and SNR to obtain higher temporal resolution.⁴ Due to the increase in SNR, more activated or deactivated brain areas could potentially be discovered. Due to the higher SNR at the head superficial area, a flexible head coil would be ideal for imaging the vessels located in the subcutaneous tissue of the galea and diagnosing cranial artery inflammation.⁵

¹Department of Radiology, Shuguang Hospital Affiliated with Shanghai University of Traditional Chinese Medicine, Shanghai, China

²Department of Diagnostic Radiology, City of Hope Medical Center, Duarte, CA, USA

*Corresponding author: Department of Radiology, Shuguang Hospital Affiliated with Shanghai University of Traditional Chinese Medicine, 528, Zhangheng Road, Shanghai 201203, China. E-mail: tanying2245@163.com



This work is licensed under a Creative Commons Attribution-NonCommercial-NoDerivatives International License.

©2021 Japanese Society for Magnetic Resonance in Medicine

Received: May 29, 2021 | Accepted: July 29, 2021

Few studies have focused on the difference in image quality between the rigid and flexible coils for the same body part in adults. The results of Bittersohl et al. showed that a flexible surface coil obtained better image quality than a rigid coil in imaging of the wrist.⁶ In the study of Gradl et al., the mean SNR was 3.5-fold higher on average with a dedicated surface coil in dental imaging compared with a rigid head and neck coil.⁷ Yeh et al. created a 7-channel flexible form-fitting MRI receiver array head coil assembled with individual coil modules, and the maximum and average SNR exceeded those from commercial 32-channel head and 4-channel flexible coil arrays by 2.63/1.35-fold and 3.89/1.50-fold, respectively.⁸ These studies focused on structural imaging; however, the performance of flexible surface coils in diffusion weighted imaging (DWI) and other functional imaging sequences used in neuroradiology remains to be determined.

Based on the above, we hypothesized that a flexible head coil would obtain better image quality. We designed a flexible head coil, tested the image performance of this coil, and compared the structural and functional images obtained from the flexible and rigid head coils.

Materials and Methods

MRI sequence and parameters

Phantom study

All the images studies were performed on the UIH 1.5 T system (United Imaging Healthcare, Shanghai, China). Three head coils were included: (1) a flexible 12-channel coil (HFC12) (Fig. 1), (2) rigid 24-channel coil (HRC24), and (3) rigid 16-channel coil (HRC16). A spherical phantom with a diameter of 17 cm (filled with 1.24-g/L NiSO₄·6H₂O and 2.60-g/L NaCl) was used for imaging, which simulated the signal intensity properties of the human brain (T₁ = 314 ms and T₂ = 267 ms) according to the State Food and Drug Administration of the People's Republic of China YY/T 0482-2010 standard.⁹

Single-slice images were obtained in the transverse, sagittal, and coronal planes, which were placed through the center point of the spherical phantom. The parameters of the single sequence were as follows: (1) T₁-weighted image (T₁WI): spin echo (SE) sequence, TR/TE = 500 ms/12.7 ms, bandwidth (BW) = 120 Hz/pixel, flip angle = 70°, FOV = 180 mm × 180 mm, matrix = 448 × 448, and slice thickness = 5 mm. (2) T₂-weighted image (T₂WI): SE sequence, TR/TE = 5000 ms/108.8 ms, BW = 190 Hz/pixel, flip angle = 90°, FOV = 180 mm × 180 mm, matrix = 448 × 448, and slice thickness = 5 mm. (3) DWI: echo planar imaging (EPI) sequence, and TR/TE = 6044 ms/134.2 ms, BW = 1480 Hz/pixel, FOV = 180 mm × 180 mm, matrix = 128 × 128, slice thickness = 5 mm. The same sequences were used in these three coils. A noise-only reference scan was obtained for each coil, which was used to calculate the SNR and the noise correlation matrix. The noise data were collected by a

gradient-recalled echo (GRE) sequence with the same position, resolution, and pixel bandwidth of T₁WI, T₂WI, and DWI, but the excitation flip angle was set to zero.

To prevent vortex artifacts, the phantom was statically positioned in the center of the coil for 10 mins before the scan started. The images were obtained by scanning the same plane twice, and the time interval between the end of the first scan and the beginning of the second scan was less than 5 mins. There was no adjustment or calibration during the two scans.

In vivo study

This study was approved by the institutional review board of Shuguang Hospital affiliated with Shanghai University of Traditional Chinese Medicine (approved No. 2017-570-53-01) according to the Declaration of Helsinki and registered with the China Clinical Trials Registry (ChiCTR1800015692). The subject signed informed consent forms.

One healthy male subject underwent a head scan with HFC12, HRC24, and HRC16. To maintain the same head position in the same sequence with different coils, the scanning slices need to be strictly selected. First, the head of this subject was placed in the center of each coil and fixed with a foam pad. In the transverse image, the center slice was selected in the line connecting the anterior and posterior commissures. In the sagittal image, the slice was selected by the center of the head and parallel to the cerebral falx. In the coronal image, the slice was parallel to the anterior margin of the brainstem.

The imaging parameters of T₁WI, T₂WI, and DWI in the transverse, sagittal, and coronal planes were as follows: (1) T₁WI: SE sequence, TR/TE = 550 ms/12.6 ms, BW = 120 Hz/pixel, flip angle = 70°, slice thickness/slice gap = 5 mm/1 mm, FOV = 200 mm × 230 mm, and matrix = 256 × 256. (2) T₂WI: fast SE sequence, TR/TE = 5000 ms/85.32 ms, BW = 190 Hz/pixel, flip angle = 90°, slice thickness/slice gap = 5 mm/1 mm, FOV = 200 mm × 230 mm, and matrix = 278 × 320. (3) DWI: EPI sequence, TR/TE = 4578 ms/107.7 ms, BW = 1510 Hz/pixel, flip angle = 90°, slice thickness/slice gap = 5 mm/1 mm, FOV = 230 mm × 230 mm, and matrix = 128 × 128. The GRE sequence with the same parameters of T₁WI, T₂WI, and DWI, with the excitation flip angle set to zero, was obtained.

SNR and noise correlation matrix

The method of multichannel combination used in both phantom and *in vivo* image reconstruction processes is the so-called sum-of-square method, which was proposed by Roemer et al.¹⁰ in 1990. Each pixel value is the square root of the sum of the squares of the pixel values corresponding to the individual coils in the array. The SNR was measured from the signal sequence data and noise sequence data. The noise sequence data were acquired from the GRE sequence with the same position, resolution, and bandwidth of the

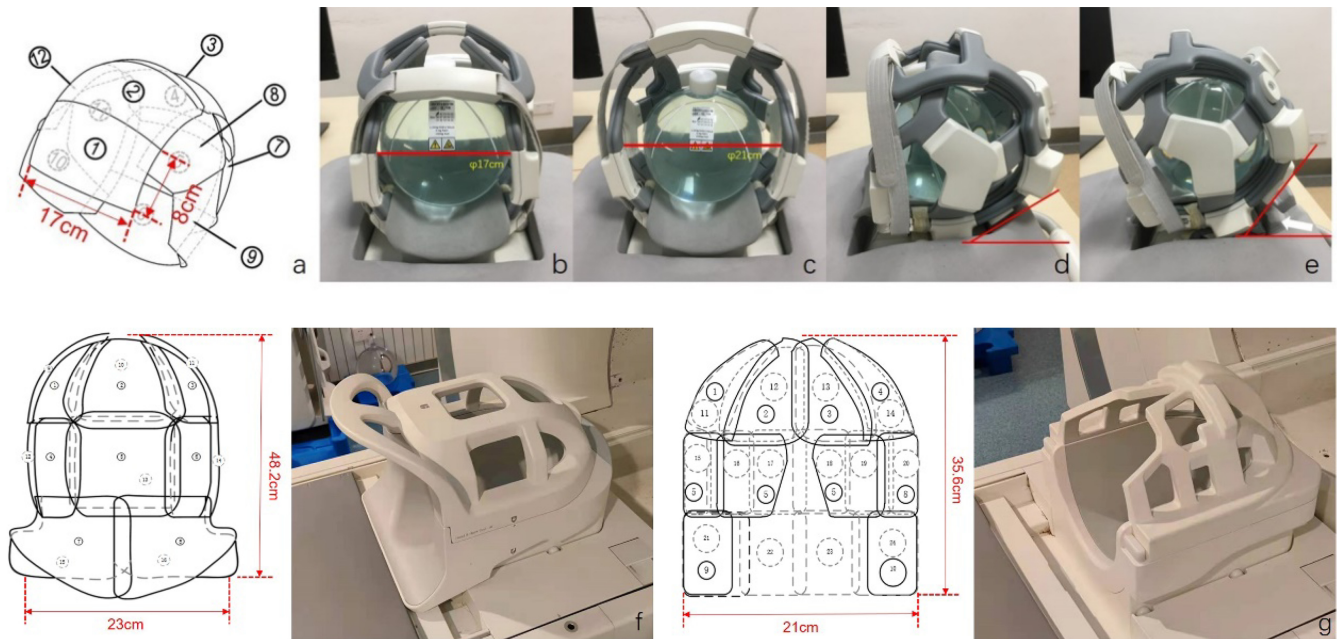


Fig. 1 The structure and configuration of the new 12-channel flexible head coil: 3D structure diagram (a). Unit 1 in the HFC12 diagram has a long diameter of 17 cm and a short diameter of 8 cm (b). The coil and the spherical phantom had a diameter of 17 cm. The inner diameter can be adjusted from a 17–21-cm ear-to-ear distance (b and c). The coil can be raised at a certain angle to adapt to different positions (d and e). 3D structure and configuration of the 16-channel and 24-channel rigid head coils (f and g). The HRC16 has a 23-cm ear-to-ear distance and 48.2 cm from the top of the head. The HRC24 has a 21-cm ear-to-ear distance and 35.6 cm from the top of the head. HFC12, 12-channel flexible head coil; HRC16, 16-channel rigid head coil; HRC24, 24-channel rigid head coil.

signal sequence data. When the flip angle was set to 0° with no RF pulses, the correlation coefficient of each unit of the coil was calculated.^{10,11} The noise correlation matrix was computed according to SE T1WI. SNR maps were obtained on a pixel-by-pixel basis from the raw k-space data and noise correlation matrix. The slices were passed through the center of the phantom and the subject in each orientation.

The SNR was calculated by the formula:

$$\text{SNR} \propto \frac{S'_{rx} \cdot S_{rx}}{\sqrt{S'_{rx} \cdot R \cdot S_{rx}}}$$

For the derivation of the specific formula, please refer to the supplementary materials. S_{rx} represents the complex image intensity received by the coil unit. R is the noise equivalent resistance matrix. S'_{rx} is the conjugate weighting coefficient.

SNR profiles

The SNR profiles were created with MATLAB (The Mathworks, Natick, MA, USA).^{12,13} The SNR profiles of each voxel in the cross-center line in transverse, sagittal, and coronal orientations were taken on SE T1WI and SE T2WI. In clinical applications, DWI is mostly used in the transverse orientation. Therefore, the SNR profile of DWI was only drawn in the transverse orientation. The phase-encoding direction was selected as right-to-left (R-L) in the transverse image, anterior-to-posterior (A-P) in the sagittal image, and R-L in the coronal image.

G-factor

The acceleration ability evaluation was based on the g-factor calculation in the phantom study. Parallel imaging was performed with sensitivity encoding (SENSE), and its reconstruction performance was evaluated by determining geometry (g) factors with the method described by Pruessmann et al.¹⁴ The acceleration direction was selected as R-L and A-P in the transverse image, A-P and head-to-foot (H-F) in the sagittal image, and R-L and H-F in the coronal image. The acceleration rate (R) was set to two and three. The g-factor maps were plotted as inverse g-factors ($1/g$) to avoid SNR loss caused by data reduction.

Results

Phantom study

The noise correlation matrix in the phantom study showed that the maximum values were 0.44, 0.45, and 0.51 for HFC12, HRC16, and HRC24, respectively. The mean values were 0.17, 0.12, and 0.10 for HFC12, HRC16, and HRC24, respectively (Fig. 2a).

The SNR profiles are shown in Fig. 3. Among the three coils, the SNR of HFC12 was the highest. The SNR of HRC16 was relatively uniform; HRC24 showed a higher SNR near the apex, while HFC12 showed a higher SNR near the edge of the coil.

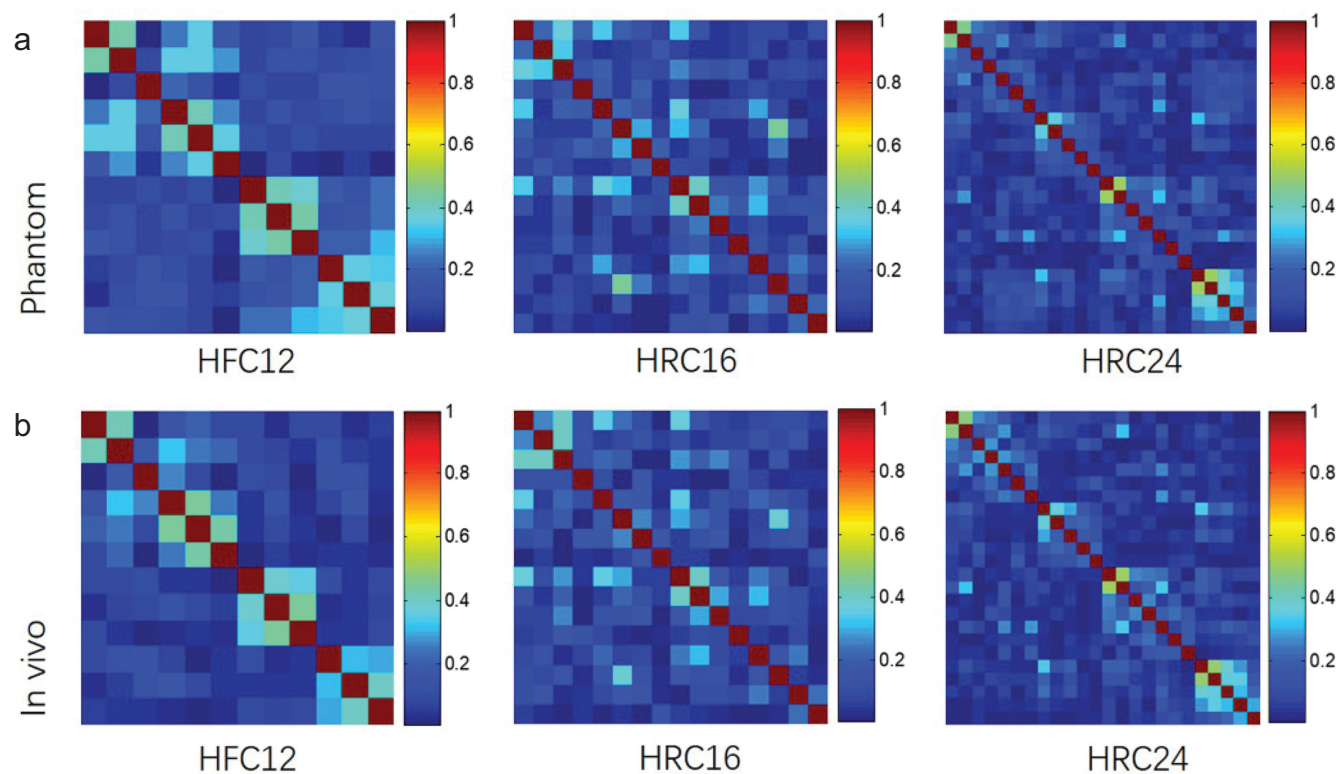


Fig. 2 The noise correlation matrix of HFC12, HRC16, and HRC24 in the phantom study (a). The maximum values were 0.44, 0.45, and 0.51 for HFC12, HRC16, and HRC24, respectively. The mean values were 0.17, 0.12, and 0.10. The noise correlation matrix in the *in vivo* study (b). The maximum values were 0.45, 0.40, and 0.50, respectively. The mean values were 0.13, 0.12, and 0.09, respectively. HFC12, 12-channel flexible head coil; HRC16, 16-channel rigid head coil; HRC24, 24-channel rigid head coil.

The SNR profiles showed that the SNR of HFC12 was the highest in the center of the coil in transverse, sagittal, and coronal images. The SNR profiles of HFC12 and HRC24 in transverse images showed a significant reduction at the center of the image in the right-left direction, while HRC16 maintained a relatively stable SNR (Fig. 4). On transverse DWI, HFC12 showed a higher SNR than HRC24 and HRC16 at the edge of the coil. In the sagittal image, the SNR of HRC24 at the bottom and the apex of the coil was the highest, but the SNR in the center of HFC12 was higher than that of HRC24. In the coronal image, similar to that of the sagittal image, the SNR in the apex of the HRC24 coil was the highest, but in other positions of the coil, HFC12 obtained the highest SNR.

The color-coded inverse g -factor images of the three coils are displayed in Fig. 5. When the reduction factor was set as $R = 2$, the three coils could obtain better acceleration ability. When the reduction factor was set to $R = 3$, the acceleration ability was not acceptable. In the R-L and A-P acceleration directions, HRC24 yielded the highest g -factors, followed by HFC12. In the H-F phase-encoding direction, HFC12 yielded the highest g -factors.

In vivo study

The SNR maps of T1WI, T2WI, and DWI acquired by the three coils are displayed in Fig. 6. Among the three coils in the transverse, sagittal, and coronal orientations, the SNR of HFC12 was the highest, that of HRC24 was the second highest, and that of HRC16 was the lowest. As shown in the transverse images, the SNR of the cortical areas of HFC12 was higher than that of the other two coils, and only the SNR near the occipital lobe was lower than that of HRC24.

The noise correlation matrix in the *in vivo* study showed that the maximum values were 0.45, 0.40, and 0.50 for HFC12, HRC16, and HRC24, respectively. The mean values were 0.13, 0.12, and 0.09 for HFC12, HRC16, and HRC24, respectively (Fig. 2b).

Discussion

In this study, a 12-channel flexible head coil was tested and compared to commercial 16-channel and 24-channel rigid head coils. In the phantom study, the flexible coil exhibited better SNR performance and had adequate g -factors for an acceleration rate of two. The SNR profiles of HFC12 were

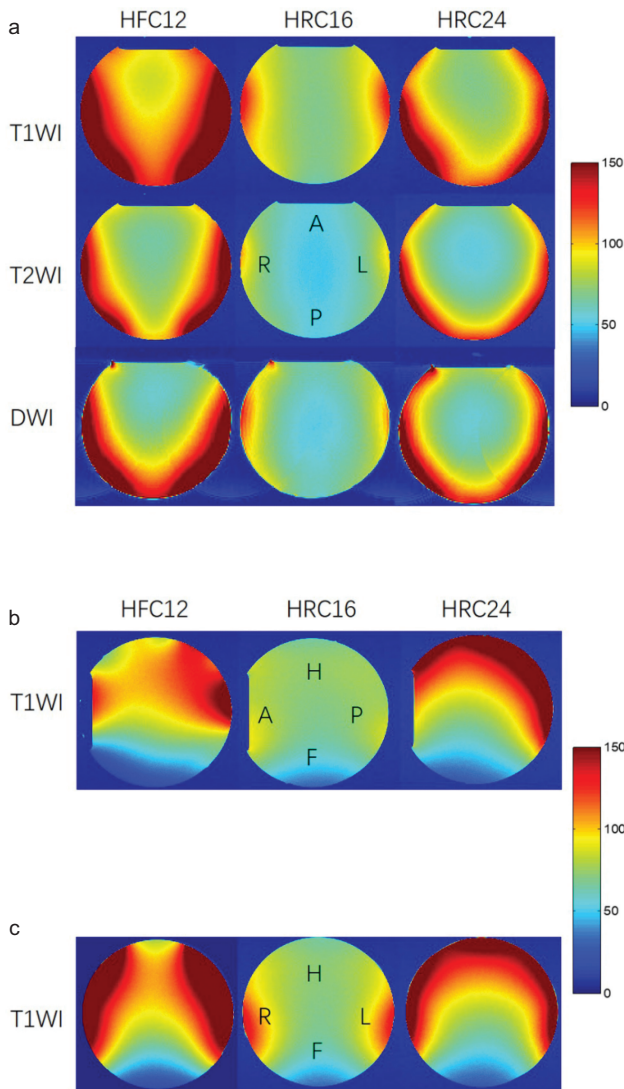


Fig. 3 Single-slice images were obtained by cutting through the phantom's central direction in transverse, sagittal, and coronal orientations. SNR maps of T1WI, T2WI, and DWI in the central transverse orientation for HFC12, HRC16, and HRC24 (a). SNR maps of T1WI in the central sagittal (b) and coronal orientation (c). Red indicates a higher SNR, and blue indicates a lower SNR. DWI, diffusion weighted imaging; HFC12, 12-channel flexible head coil; HRC16, 16-channel rigid head coil; HRC24, 24-channel rigid head coil; T1WI, T1-weighted image; T2WI, T2-weighted image.

similar to a U shape, and a higher SNR was located at the edge of the coil in both the SE and EPI sequences. In the *in vivo* study, the 12-channel flexible head coil exhibited SNR performance similar to the phantom study, and HFC12 had a higher SNR in the cortical areas than rigid coils, except for the occipital lobe.

The routine method to improve the SNR of MRIs is to increase the coil units.¹⁵ A higher SNR may be acquired

with more coil channels.¹³ Compared with 16-channel and 24-channel commercial head coils, the new flexible head coil array has fewer coil units or channels. The 12-channel flexible head coil was designed by shortening the distance between the coil and the target, which could closely fit the heads of different sizes and meet the needs of specific imaging applications. Fewer coil units simplifies the design and reduces the coupling effect due to the increasing number of elements.¹⁶

Although the number of units was decreased, the flexible head coil obtained a better SNR than the rigid coil with more coil units. In the phantom study, the SNR profiles showed that HFC12 obtained a better SNR, especially at the edge of the coil. However, at the bottom and the apex of the coil, HRC24 gained the highest SNR. The reason might be that most coil units of HRC24 were located in the bottom and the apex of the coil, which obviously increased the SNR. The acceleration ability of HFC12 was slightly lower than that of HRC24 in the R-L and A-P acceleration directions under a reduction factor of two. In the H-F acceleration direction, the acceleration ability of HFC12 was the best, which may be explained by the unit density of the coil. HRC16 has four units in the neck position, the same as HFC12, but the coverage of HRC16 is larger. Therefore, the unit density of HRC16 is lower than that of HFC12 due to the lower acceleration ability. In the R-L and A-P acceleration directions, the coil unit density of HRC24 is the highest, followed by HFC12. In the H-F acceleration direction, there are fewer units in the upper part of HRC24, so the acceleration ability in the H-F acceleration direction should be slightly worse than that of HFC12. When the reduction factor was set to 3, the acceleration ability was unacceptable in the three coils because the coil unit density did not support it.

In the *in vivo* study, the SNR of the brain areas close to the coil was significantly increased. The coil units of HFC12 were uniformly distributed and could be tightly wrapped to the head so that the SNR of the cortex could be greatly improved, which suggested that HFC12 might be more adaptive to studies focused on cortical areas. When the size of the head was small, some areas, such as the forehead, were far away from the coil with fixed size, which made the SNR of the frontal lobe decrease obviously. Similar to the results of the phantom study, HRC24 showed the highest SNR in the occipital lobe among the three coils due to its structure.

Previous studies have reported that surface coils might obtain better image quality than volume coils.^{6,7,17} Lopez Rios et al. designed an adjustable 13-channel head coil, for which the average SNR was increased by 68% and the SNR of the cortex was increased by 122% compared with the commercial 32-channel head coil in the phantom test.¹⁸ Similar to Lopez Rios et al., our flexible coil also exhibited a much higher SNR in the cortex than rigid coils. This is especially important for EPI sequences because EPI sequences are commonly used in fMRI. In fMRI, the temporal SNR is particularly important, which puts forward

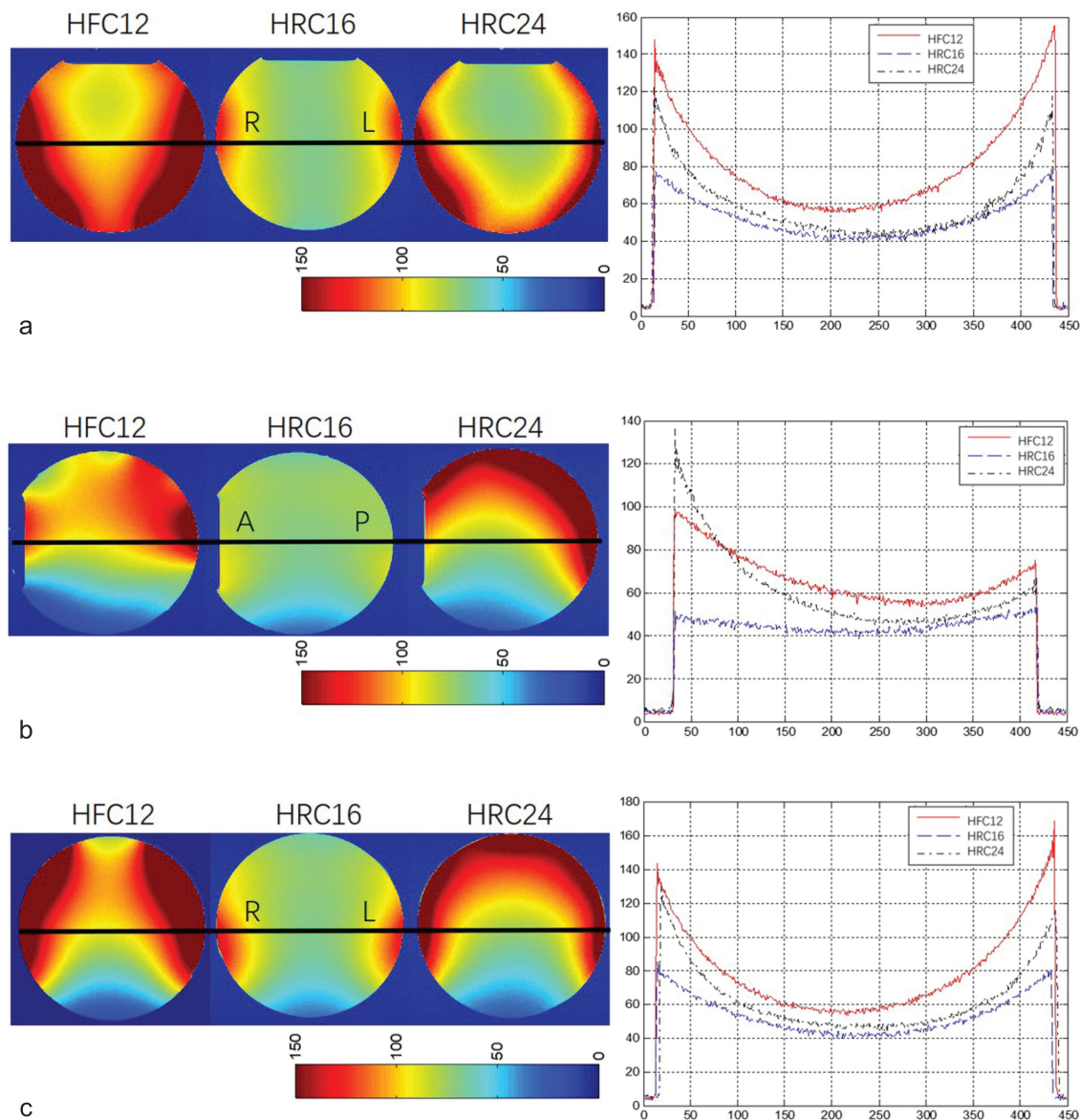


Fig. 4 The SNR profiles were made from T1WI of the three coils. A single-slice image cut through the center of the phantom in different orientations. The SNR profile was selected to pass the R-L direction in the transverse (a), A-P direction in the sagittal (b), and R-L direction in the coronal (c) directions. The red line represents HFC12, the blue line represents HRC16, and the black line represents HRC24. The longitudinal coordinate presents the SNR value of every voxel, and the horizontal coordinate presents the location of the voxel. A-P, anterior-to-posterior; HFC12, 12-channel flexible head coil; HRC16, 16-channel rigid head coil; HRC24, 24-channel rigid head coil; R-L, right-to-left; T1WI, T1-weighted image.

higher requirements for the SNR of time series data and signal stability. A time series of images with a high SNR is required to detect activation-related signal changes.¹⁹ In EPI-DWI sequences, our study showed the advantages of flexible coils in SNR, and the ability of HFC12 in fMRI should be tested in the future.

In addition, the SNR might also be affected by the position of the imaging object in the flexible coil and the distribution of channels in the HFC coil. Some research

has shown that a surface coil can obtain good SNR and image uniformity within a depth equal to its radius.²⁰ The attenuation is lower when the signal is transmitted at the center of the coil.²¹ Therefore, the SNR near the center of the coil is often lower than that near the surface. This should be considered in the utilization of this coil in the clinical environment.

There are some limitations in this study. First, the *in vivo* study was performed in one healthy subject. Although

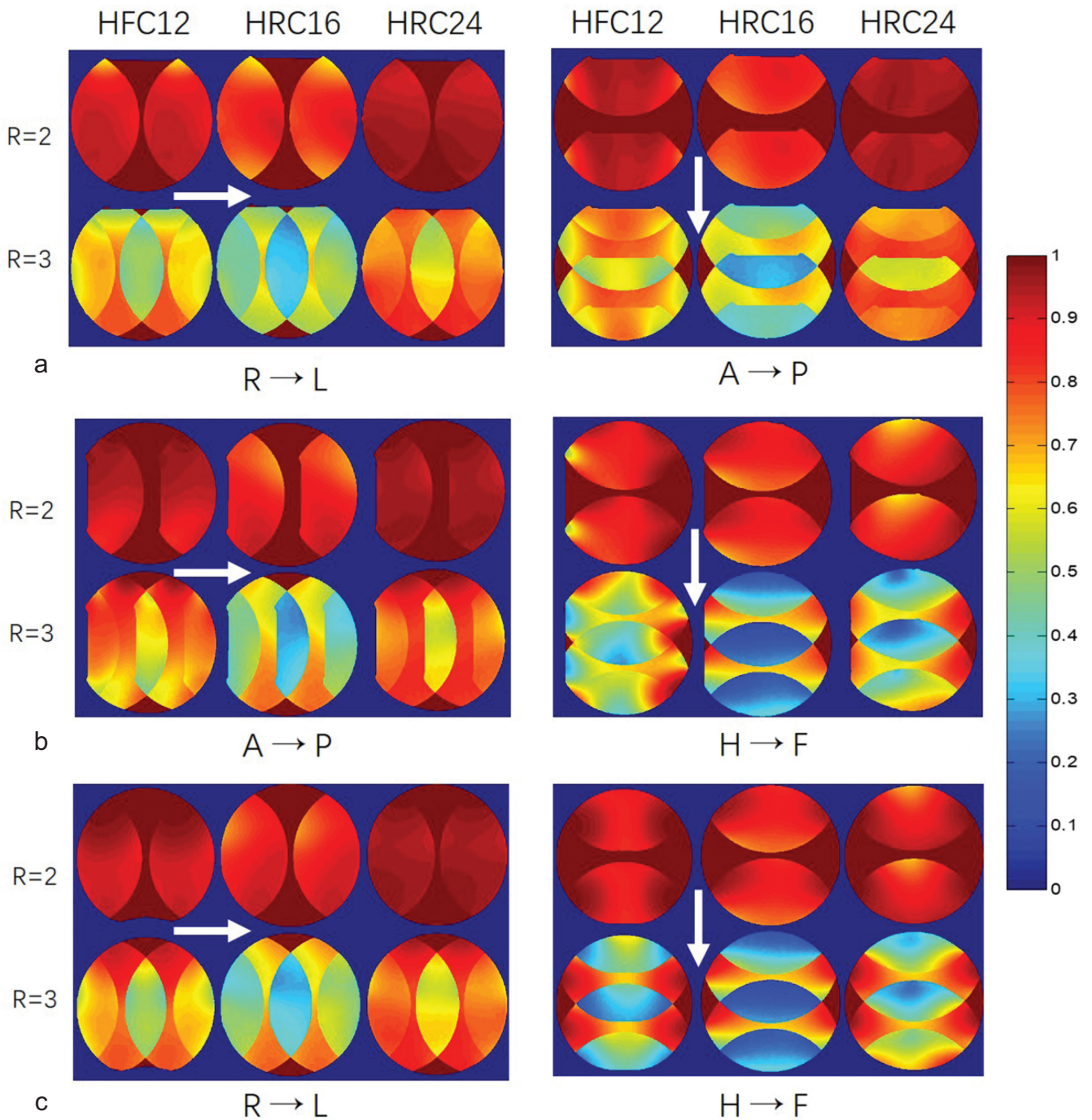


Fig. 5 The $1/g$ -factor maps of the three coils were made from a T1WI single-slice image in different orientations (**a** for transverse direction; **b** for sagittal direction; **c** for coronal direction). The reduction factors were selected to be 2 and 3. The acceleration directions are shown as white arrows. A-P, anterior-to-posterior; H-F, head-to-foot; HFC12, 12-channel flexible head coil; HRC16, 16-channel rigid head coil; HRC24, 24-channel rigid head coil; R-L, right-to-left; T1WI, T1-weighted image.

multiple subjects were helpful to test the repeatability of coil performance, the important evaluation method of coils was the phantom study. Second, the study did not reflect the advantages of this coil in patients with disease, so a study should be designed to ensure the ability of this HFC12 to

identify brain lesions in the future. The flexible head coil was relatively soft, and the coil was checked to ensure integrity before every MR examination. It is necessary to find the type of material to strengthen this coil. In addition, this coil was designed for 1.5 T MR scanners, and all of the tests were

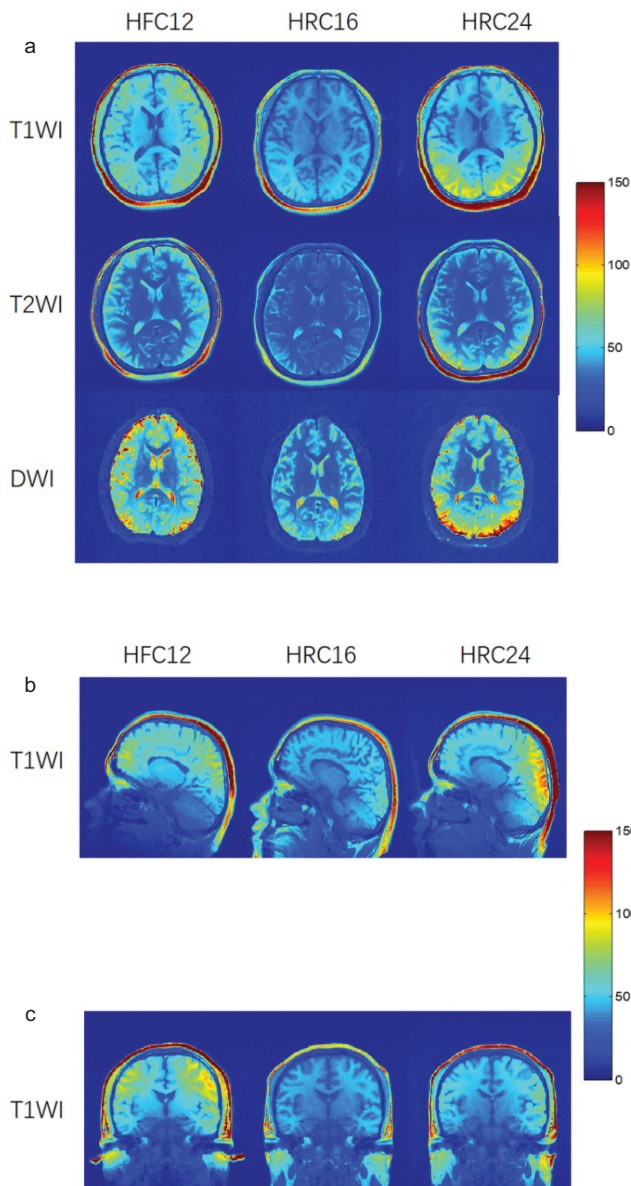


Fig. 6 SNR maps in the *in vivo* study. A single central-slice image was obtained in transverse, sagittal, and coronal orientations. SNR maps of T1WI, T2WI, and DWI in the central transverse orientation for HFC12, HRC16 and HRC24 (a). SNR maps of T1WI in the central sagittal (b) and coronal orientation (c). Red indicates a higher SNR, and blue indicates a lower SNR. DWI, diffusion weighted imaging; HFC12, 12-channel flexible head coil; HRC16, 16-channel rigid head coil; HRC24, 24-channel rigid head coil; T1WI, T1-weighted image; T2WI, T2-weighted image.

performed on a 1.5 T MR system. However, 3 T MR scanners are currently very widely used.^{17,22,23} In the future, flexible head coils that can be used on a 3 T MR system should be developed, and better image quality might be obtained. The acceleration ability was not satisfactory until now, and this should be evaluated in future studies. Although we confirmed the value of the coil in the EPI-DWI sequence,

the imaging sequence of the central neural system still included blood oxygen level-dependent (BOLD) fMRI and diffusion tensor imaging. The application value of HFC12 in these fields should be explored in future studies.

Conclusion

The new flexible head coil has fewer coil units and can be adjusted appropriately. This improves the SNR in both the SE and EPI sequences compared with commercial rigid head coils, especially at the cortical area. HFC12 might be more adaptive to studies focused on cortical areas.

Funding

This work was supported by the Shanghai Science and Technology Committee [17441902600, 18401970300]; and Shanghai Traditional Chinese Medicine school [XingLin Scholar plan, No. ZDCG701 and No. SGZXY201909].

Acknowledgments

JunAn Zheng and XianWen Fan provided the technical support for the phantom test.

Conflicts of Interest

All authors report no conflicts of interest in relation to the materials or methods or findings in this study.

Supplementary Materials

A supplementary file is available online.

References

1. Gruber B, Froeling M, Leiner T, et al. RF coils: a practical guide for nonphysicists. *J Magn Reson Imaging* 2018; 48:590–604.
2. Corea JR, Lechene PB, Lustig M, et al. Materials and methods for higher performance screen-printed flexible MRI receive coils. *Magn Reson Med* 2017; 78:775–783.
3. Corea JR, Flynn AM, Lechène B, et al. Screen-printed flexible MRI receive coils. *Nat Commun* 2016; 7:10839.
4. Scouten A, Papademetris X, Constable RT. Spatial resolution, signal-to-noise ratio, and smoothing in multi-subject functional MRI studies. *Neuroimage* 2006; 30:787–793.
5. Franke P, Markl M, Heinzlmann S, et al. Evaluation of a 32-channel versus a 12-channel head coil for high-resolution post-contrast MRI in giant cell arteritis (GCA) at 3T. *Eur J Radiol* 2014; 83:1875–1880.
6. Bittersohl B, Huang T, Schneider E, et al. High-resolution MRI of the triangular fibrocartilage complex (TFCC) at 3T: comparison of surface coil and volume coil. *J Magn Reson Imaging* 2007; 26:701–707.
7. Gradl J, Höreth M, Pfefferle T, et al. Application of a dedicated surface coil in dental MRI provides superior image

- quality in comparison with a standard coil. *Clin Neuroradiol* 2017; 27:371–378.
8. Yeh JT, Lin JL, Yi-Tien Li, et al. A flexible and modular receiver coil array for magnetic resonance imaging. *IEEE Trans Med Imaging* 2019; 38:824–833.
 9. YY/T 0482-2010. Technical requirements and test methods for magnetic resonance equipment for medical diagnosis. Beijing: State Food and Drug Administration, 2010.
 10. Roemer PB, Edelstein WA, Hayes CE, et al. The NMR phased array. *Magn Reson Med* 1990; 16:192–225.
 11. Kellman P, McVeigh ER. Image reconstruction in SNR units: a general method for SNR measurement. *Magn Reson Med* 2005; 54:1439–1447.
 12. Yuan ZL, Zhang ZX, Qiu JF, et al. Performance comparison of different MRI radio-frequency coils based on ACR phantom. *China Medical Devices* 2015; 30:100–103.
 13. Reiss-Zimmermann M, Gutberlet M, Köstler H, et al. Improvement of SNR and acquisition acceleration using a 32-channel head coil compared to a 12-channel head coil at 3T. *Acta Radiol* 2013; 54:702–708.
 14. Pruessmann KP, Weiger M, Scheidegger MB, et al. SENSE: sensitivity encoding for fast MRI. *Magn Reson Med* 1999; 42:952–962.
 15. Li Y, Lee J, Zhang L, et al. Design and testing of a 24-channel head coil for MR imaging at 3 T. *Magn Reson Imaging* 2019; 58:162–173.
 16. Parikh PT, Sandhu GS, Blackham KA, et al. Evaluation of image quality of a 32-channel versus a 12-channel head coil at 1.5T for MR imaging of the brain. *AJNR Am J Neuroradiol* 2011; 32:365–373.
 17. Wong OL, Yuan J, Yu SK, et al. Image quality assessment of a 1.5T dedicated magnetic resonance-simulator for radiotherapy with a flexible radio frequency coil setting using the standard American College of Radiology magnetic resonance imaging phantom test. *Quant Imaging Med Surg* 2017; 7:205–214.
 18. Lopez Rios N, Foias A, Lodygensky G, et al. Size-adaptable 13-channel receive array for brain MRI in human neonates at 3 T. *NMR Biomed* 2018; 31:e3944.
 19. Parrish TB, Gitelman DR, LaBar KS, et al. Impact of signal-to-noise on functional MRI. *Magn Reson Med* 2000; 44:925–932.
 20. Kumar A, Bottomley PA. Optimized quadrature surface coil designs. *MAGMA* 2008; 21:41–52.
 21. Wright SM, Wald LL. Theory and application of array coils in MR spectroscopy. *NMR Biomed* 1997; 10:394–410.
 22. Winkler SA, Corea J, Lechêne B, et al. Evaluation of a flexible 12-channel screen-printed pediatric MRI coil. *Radiology* 2019; 291:180–185.
 23. Wiggins GC, Triantafyllou C, Potthast A, et al. 32-channel 3 Tesla receive-only phased-array head coil with soccer-ball element geometry. *Magn Reson Med* 2006; 56:216–223.